A Semi-Powered Ankle Prosthesis and Unified Controller for Level and Sloped Walking

Harrison L. Bartlett, Shane T. King, Michael Goldfarb, *Member, IEEE*, and Brian E. Lawson, *Member, IEEE*

***Abstract*— This paper describes a semi-powered ankle prosthesis and corresponding unified controller that provides biomimetic behavior for level and sloped walking without requiring identification of ground slope or modulation of control parameters. The controller is based on the observation that healthy individuals maintain an invariant external quasi-stiffness (spring like behavior between the shank and ground) when walking on level and sloped terrain. Emulating an invariant external quasi-stiffness requires an ankle that can vary the set-point (i.e., equilibrium angle) of the ankle stiffness. A semi-powered ankle prosthesis that incorporates a novel constant-volume power-asymmetric actuator was developed to provide this behavior, and the unified controller was implemented on it. The device and unified controller were assessed on three subjects with transtibial amputations while walking on inclines, level ground, and declines. Experimental results suggest that the prosthesis and accompanying controller can provide a consistent external quasi-stiffness similar to healthy subjects across all tested ground slopes.**

***Index Terms*— Prostheses, amputation, design, control, ankle, biomechanics.**

I. Introduction

THE current state of the art in ankle-foot prostheses is a leaf-spring-like device typically constructed from carbon fiber. These devices act as a spring about a constant neutral set point (equilibrium resting position of the spring). While passive leaf-spring-like prosthetic ankles perform well during the stance phase of level ground walking, they lack the behavioral adaptability to accommodate other terrains or activities. Several studies illuminate the challenges of non-level walking as an individual with a transtibial amputation (ITTA) [1]–[8]. In one study [2], 76% of the ITTAs surveyed indicated that they were able to walk unassisted outside on level ground while only 48% could walk unassisted outside on uneven ground, highlighting the difficulty posed by non-level terrain. The challenges of walking on sloped ground are also highlighted by [1] in which subjects indicated that socket comfort during sloped walking was significantly worse than that of level walking, presumably due to the incongruent angles of the ground slope and the ankle set point during stance phase.

Manuscript received September 14, 2020; revised December 3, 2020; accepted December 29, 2020. Date of publication January 5, 2021; date of current version March 2, 2021. This was work supported by NIH under Grant 1R43HD096967-01. *(Corresponding author: Harrison L. Bartlett.)*

The authors are with the Department of Mechanical Engineering, Vanderbilt University, Nashville, TN 37212 USA (e-mail: harrison.logan.bartlett@gmail.com).

Digital Object Identifier 10.1109/TNSRE.2021.3049194

Recently, fully powered prostheses have been developed to address this lack of versatility [9]–[22]. The behavior of these fully powered devices is software-controllable and can, therefore, be adapted to different scenarios such as uneven terrain [23], sloped terrains [24] or walking up and down stairs [25]–[27].

In order to provide the adaptability offered by powered prostheses in a potentially smaller, lighter, and quieter package, computer-controlled, primarily passive devices have recently been developed in both the academic and industrial settings [28]–[33]. These primarily passive devices rely on energetically passive mechanisms such as springs and dampers during the load-bearing phases of gait with low-power actuators to modulate the passive parameters of these elements. The utilization of passive mechanisms allows for a reduction in size, mass, and power consumption relative to fully powered devices. This primarily passive (semi-powered) class of device includes prostheses such as Ossur's Proprio Foot and the device developed in [33] which use a nonbackdrivable actuator to change the set point of a carbon fiber spring during the swing phase of gait. These nonbackdrivable mechanisms allow for the prosthesis to adjust to variations in global slope of the ground (by changing the set point of the ankle) over the course of multiple strides while maintaining the stance-phase behavior of the leaf-spring-like standard of care. These repositioning devices also actively dorsiflex the ankle during the swing phase of gait, thereby mitigating the risk of foot scuffing or stumbles [34], [35]. Due to the nonbackdriveable nature of these devices however, they lack the ability to conform to the shape of the terrain each step (they can only change the ankle set point while the ankle is unloaded). As such, they are unable to adapt to locally uneven terrain or adapt quickly to globally sloped terrain, and as a result can also increase the time between heel strike and foot flat, thereby decreasing stability [36].

Another common variant of the primarily passive prosthetic ankle is the modulated damping prosthesis. This class of primarily passive device includes multiple commercially available prostheses such as the Meridium (Ottobock), Raize (Fillauer), Triton Smart Ankle (Ottobock), Kinnex (Freedom Innovations), and the Elan (Endolite). These modulated damping devices provide a computer-controlled level of damping about the ankle joint within a range of ankle angles, then provide a stiffness outside of that range. Due to their damper behavior, these prostheses can adapt to the slope of the terrain on each step, which may increase socket comfort for ITTA

users [1]. However, due to the lack of a mid-stance stiffness, these devices may compromise mid-stance stability (spring-like restoring torques during mid-stance) as well as terminal-stance energy return.

In order to provide slope adaptation, some researchers have developed passive devices that alter the ankle stiffness set-point as a function of ground slope [37]–[39]. These devices incorporate mechanical or hydraulic locking mechanisms to lock the ankle joint at various ankle angles as a function of ground slope. While this approach has shown promise, the implementation of passive, slope-adaptive locking is a challenge, and in general lacks the adaptability of a computer-controlled device.

This paper presents the design and control of an ankle prosthesis intended to provide ground-adaptive behavior with the same essential mid-stance stiffness-like behavior as observed in healthy individuals. In particular, as observed in healthy individuals and described in this paper, the essence of ground-adaptive behavior is an invariant external quasi-stiffness (spring-like relationship between ankle torque and shank angle) during mid-stance, preceded by a conformal damping behavior during early stance. In order to provide this behavior, the authors have designed an ankle/foot prosthesis that can provide conformal damping during plantarflexion and can also lock the ankle at a selectable angle (thereby changing the set point of a compliant foot spring). This behavior, in combination with a passive compliant foot, provides the essential ground-adaptive behavior observed in healthy individuals. Further, in order to reset the ankle between strides, the prosthesis additionally incorporates a small motor, which resets ankle angle during swing phase. The authors describe the design of the prosthesis and show data on three individuals with transtibial amputation that indicates: 1) ground-adaptive mid-stance behavior; 2) conformal damping at heel strike; and 3) swing phase behaviors, all three of which are representative of the ground-adaptive behaviors observed in healthy individuals.

II. Prosthesis Design

The primary goal during the design of the semi-powered prosthesis presented in this work was to minimize device size and mass while simultaneously maximizing biomechanical benefit to the user. To address that goal, a set of design requirements were drafted and described in detail in [40]. These requirements are summarized as follows: 1) mass less than 1.5 kg, 2) build height less than 175 mm, 3) locking ankle torque of at least 120 Nm, 4) maximum dissipative power of 200 W, and 5) active repositioning power of 10 W.

It should be noted that the requirements dictate that the ankle should dissipate large amounts of power (200 W), but only generate small amounts of power (10 W). The positive power requirements for this ankle are not sufficient to provide a powered pushoff at terminal stance. This design choice was made in order to reduce the size and mass of this prosthesis relative to fully powered devices. Instead of using a high power actuator for the high-torque load bearing phases of gait, relatively small passive components can be utilized, thereby decreasing the size and mass of the device at the cost of high positive power capabilities. This power asymmetry was achieved in prior work through the design of a novel power-asymmetric actuator [40]–[42]. The previously presented actuator design, however, required the use of an accumulator which prevented it from providing significant resistive torques in one direction. The unidirectional capabilities of the previous actuator limited control authority during the heelstrike phase of gait and also prevented the device from providing adequate support to the user during standing. Due primarily to this limitation, the semi-powered prosthetic ankle presented in [41] was redesigned using a novel constant-volume power-asymmetric actuator.

This section presents the redesigned power-asymmetric actuator and a brief review of the remaining elements of the prosthetic ankle design which have been presented in detail in [41].

A. Constant Volume Power-Asymmetric Actuator

An ideal power asymmetric actuator is able to generate small amounts of power while being able to dissipate large amounts of power, independent of the direction of actuator force. Such power-asymmetric actuators have been used previously in the haptics field to improve the haptic rendering of discrete passive environments [43]. The power-asymmetric actuator previously designed for a prosthetic ankle in [40] utilized a small electromechanical drive system for positive power generation and a closed-system hydraulic unit in parallel for power dissipation. The hydraulic unit consisted of a single rod hydraulic cylinder with a rotary spool and sleeve damper valve in the fluid line connecting the rod and piston sides of the cylinder. To account for volume changes in the system due to rod movement, an accumulator was connected to the rod side of the cylinder.

As discussed in [44], the use of a single-rod cylinder in a closed hydraulic system introduces performance limitations relative to the use of a constant-volume actuator. Due to the introduction of an accumulator into the hydraulic circuit (which is necessary because of the volume fluctuations introduced by the movement of the rod), the hydraulic unit was only able to dissipate significant power or lock in the direction of cylinder retraction (ankle dorsiflexion). When forced in the cylinder extension direction, the actuator is only able to resist with the force generated by pressure acting on the accumulator (atmospheric pressure in this case).

This linear actuator limitation imposes constraints on the capabilities of the ankle prosthesis. Namely, the ankle is able to lock in the dorsiflexion direction but is only able to resist motion in the plantarflexion direction with a small amount of torque. Regarding activities of daily living, resistance to dorsiflexion is more prevalent than resistance to plantarflexion. To provide desirable characteristic for walking, however, the ankle should be able to provide a resistive torque in the plantarflexion direction during the heelstrike and ground conformation events of walking. This phase of gait is sometimes called "controlled plantarflexion," and without the ability to resist large torques in the plantarflexion direction, the ankle prosthesis as previously presented has limited control authority. Specifically, in the previous prototype, the ankle was only able to resist plantarflexion with an ankle torque of

approximately 1.5 Nm (due to atmospheric pressure, the cross sectional area of the rod end of the cylinder, and the moment arm of the actuator about the ankle joint). Biomechanical data from healthy subjects indicates that during the controlled plantarflexion phase of walking, the ankle resists plantarflexion with a torque of approximately 8 Nm for an 80 Kg individual [45]. As such, the previous prototype was unable to provide the requisite torque to match the performance of a healthy ankle during controlled plantarflexion. As a result, during the ground conformation phase of walking with the previous ankle prototype, rapid, uncontrolled plantarflexion (otherwise known as "foot slap") was occasionally observed. Additionally, the ankle must provide bidirectional resistance in order to provide stability to the user during quiet standing. The previous device's inability to do so was also cited by users of the previous prototype as a significant limitation.

The ankle's performance limitations may be addressed through the use of a constant volume hydraulic actuator in which the volume of fluid in the system is not a function of stroke length. The most common constant volume hydraulic actuator is a double rod cylinder (a cylinder where the rod is mirrored about the piston) in which one side of the rod exits the cylinder while the other side of the rod enters the cylinder, thereby maintaining the volume of hydraulic system as a function of stroke length. However, double rod cylinders pose problems with regard to design envelope as they require approximately twice the actuator length when compared to a single rod cylinder with equivalent stroke length. In order to provide a constant volume hydraulic actuator without the size penalties associated with a double rod cylinder, researchers have proposed alternative cylinder designs that maintain constant volume as a function of stroke length and utilize only a single rod [46]–[49]. In order to achieve a minimum actuator diameter (and thereby a minimal ankle device envelope), a novel five chamber constant volume single rod hydraulic cylinder was developed in [44] for this semi-powered ankle application. A variation of the cylinder topology presented in [44], [50] was utilized for the semi-powered ankle and can be seen schematically in Fig. 1.

This hydraulic cylinder consists of an inner cylinder nested concentrically inside of an outer cylinder. The piston assembly consists of a circular inner piston that moves within the inner cylinder and an annular piston that moves within the annular space between the inner and outer cylinders. The two pistons are then connected to one another outside of the cylinder body by a series of four rods (one central rod and three rods arranged circularly around the outer annular piston). The actuator contains fluid on the non-rod side of the cylinder in the chamber defined by the annular space between the inner and outer cylinder. The rod side of the actuator contains fluid in the annular chamber between the inner and outer cylinders as well as in the annular space between the central rod and the inner cylinder (Fig. 1). This cylinder topology is able to maintain constant fluid volume as a function of stroke length by specifying that the cross-sectional area of the fluid on the rod side of the cylinder be equal to that of the non-rod side. Because of the constant fluid volume behavior of this cylinder topology, an accumulator is no longer required, and

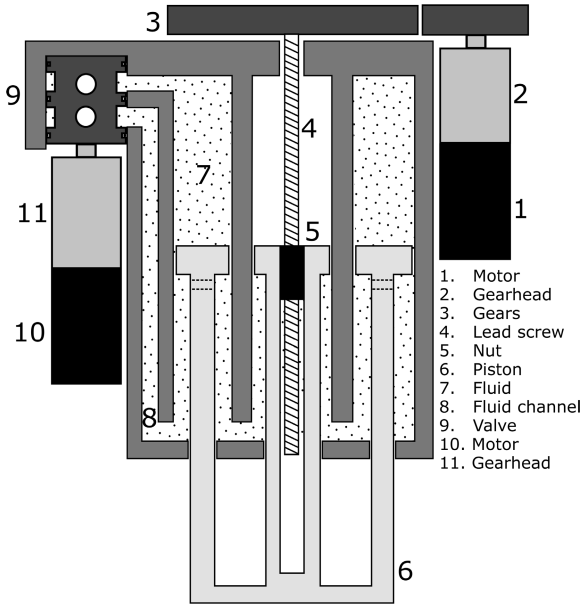

Fig. 1. Constant volume power asymmetric actuator schematic. Components are labeled within the figure The actuator includes an inner cylinder, outer cylinder, inner piston, outer piston, fluid return path (fluid channel), damping valve, a motor and gearhead for driving the valve, lead screw, lead nut, gears, and a motor and gearhead for driving the electromechanical actuator. Hydraulic fluid is contained in the regions with small dots.

the functional deficiency present in the previous design is eliminated. A variation of this cylinder topology was designed, built, and assessed in [44] where it was shown to have constant volume properties

The actuator's power dissipation capabilities are provided by a damper valve connecting the two sides of the cylinder while the positive power capabilities are provided by a small electromechanical actuator mechanically in parallel to the hydraulic unit. The damper valve unit consists of a pressure-balanced rotary spool and sleeve two-way valve driven by a 10 W brushless motor. The electromechanical actuator consists of a separate 10 W brushless DC motor driving a set of helical gears which in turn drive a lead screw. The lead screw is nested concentrically with the inner cylinder of the hydraulic unit and drives a nut which is attached to the piston assembly (Fig. 1).

B. Ankle Structure

The ankle utilizes an inverted slider-crank mechanism to transduce the linear force and motion of the actuator to rotary torque and motion of the prosthetic ankle. Additionally, the ankle structure utilizes a compliant element (steel leaf spring) to connect one end of the actuator to the structure. As such, the ankle is configured as a series elastic actuator [22], [51] in which the compliant element has a relatively small range of motion (after which the compliant element saturates). The deformation of this series spring is measured differentially by two encoders in order to provide a measurement of ankle torque as described in [41].

The prosthetic ankle device also utilizes a carbon fiber foot plate in series with the inverted slider-crank mechanism in order to provide appropriate foot stiffness and associated energy storage and return behavior during the stance phase of

Fig. 2. Assembled semi-powered prosthetic ankle. The ankle utilizes an inverted slider crank structure and the constant volume power asymmetric actuator. The ankle joint is in series with a custom carbon fiber foot plate. The custom embedded system is visible on the side of the ankle.

TABLE I
SEMI-POWERED ANKLE HARDWARE SPECIFICATION SUMMARY

Specification	Value	Units
Mass	1.35	kg
Range of Motion	42 (12 dorsi to 30 plantar)	deg
Build Height	16.3	cm
Active Power	~10	W
Passive Torque	>150	Nm

walking. The ankle connects to standard prosthetic componentry via a pyramid connector connected to the shank segment of the device. The full semi-powered ankle device utilized in this study can be seen in Fig. 2 and key hardware specifications are outlined in Table I.

C. Sensing, Electronics, and Low Level Control

The prosthetic ankle measures the valve position, actuator length, ankle joint angle, ankle torque (within the range of series elasticity), and global reference frame orientation (via an inertial measurement unit, IMU). Note the ankle torque is measured for purposes of determining heel strike and toe-off (therefore full range of torque measurement is not necessary). A custom embedded system, employing two processors (primary processor and digital signal processor) was designed for the semi-powered prosthesis. The primary processor receives position feedback from the valve and actuator motors and implements a PD position control loop outputting a reference motor current. This position control loop is cascaded with a current control loop which is implemented in the digital signal processor. High level position commands for the valve and drive motor are generated in MATLAB Simulink and communicated to the embedded system via a CAN bus. High level control was implemented in MATLAB Simulink in order to facilitate rapid control development. A detailed description of this hierarchical control structure as well as an overview of the sensing (specific sensors) and embedded system design/architecture can be found in [41].

III. UNIFIED WALKING CONTROLLER DESIGN

Some previous approaches for controlling prostheses over sloped terrains have involved the identification of the ground slope on each step (e.g., [24]). Ground slope identification, however, suffers from drawbacks in that foot shells used on prosthetic devices as well as shoes introduce compliance between the foot and the ground, making accurate slope identification difficult. In this section, the authors describe the development of a single control policy for a semi-powered prosthetic ankle that allows for walking on globally sloped terrain (inclines and declines) without identifying the ground slope. The controller leverages the idea of maintaining a consistent external quasi-stiffness of the shank across varying ground slopes.

A. External Quasi-Stiffness

External quasi-stiffness is defined as the spring-like relationship between a body segment and an orientation in the global reference frame. Specifically, in [23], it was shown that healthy subjects maintain a consistent external quasi-stiffness (slope of the ankle torque vs. shank angle plot) during the mid-stance phase of walking across uneven terrain, independent of the local ground slope. In other words, during uneven terrain walking, the ankle acts to enforce a spring-like behavior between the shank body segment and the gravity vector. This insight was leveraged to develop a controller for a powered prosthesis in which this external quasi-stiffness was virtually enforced to enable uneven terrain walking on the device [23].

Although evidence suggests that this property of external quasi-stiffness is maintained across changes in local slope, the degree to which external quasi-stiffness is maintained across changes in global slope remained unclear. To address this question, data from [45] were examined to determine the consistency of the external quasi-stiffness across these trials. The data analyzed consisted of ten healthy subjects (mean subject mass of 69 $\pm$ 14 Kg) walking on slopes ranging from -6 to 6 deg in 3 deg increments at a walking speed of 0.8 m/s. The ankle angle was plotted against body mass normalized ankle torque during the middle stance phase of gait to depict the ankle joint internal quasi-stiffness during stance (Fig. 3a). Additionally, the angle of the shank segment relative to the gravity vector (shank angle) was plotted against body mass normalized ankle torque for the middle stance phase of walking (Fig. 3b) in order to depict the external quasi-stiffness.

Trajectories in Fig. 3 begin at the left-most position on the plot and follow the curve from left to right. Fig. 3a shows that the ankle joint quasi-stiffness is relatively inconsistent across changes in ground slope. In contrast, as can be seen from Fig. 3b, the trajectories for walking on these various slopes are fairly aligned when viewed as an external quasi-stiffness. These trajectories form a consistent external quasi-stiffness (when characterized by a best-fit linear regression) with approximately the same shank-based equilibrium angle (approximately zero deg shank angle or aligned with the gravity vector) and quasi-stiffness (slope of the trajectory). The quasi-stiffness consistency was measured by the range of the torque zero-crossings. The width of the torque zero-crossings (gray band in Fig. 3) was 12 deg and 5 deg for the internal and external quasi-stiffness data, respectively. Additionally, the root mean squared error (RMSE) was calculated relative to a best-fit line for the internal quasi-stiffness data (Fig. 3a)

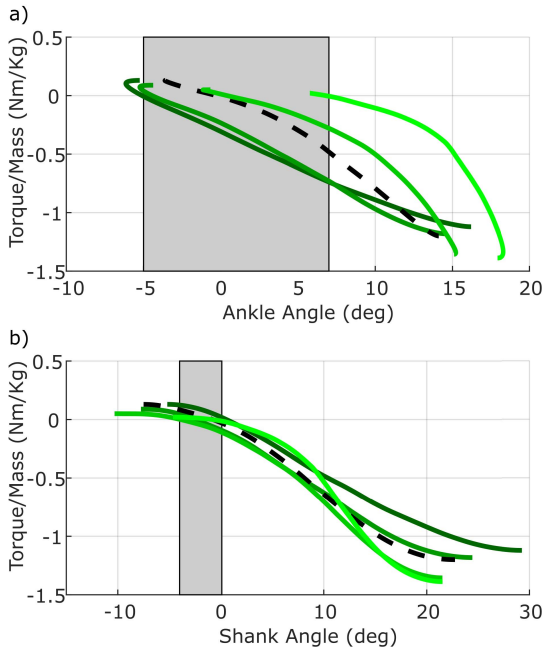

Fig. 3. Ankle torque during mid stance plotted against ankle angle (a) and shank angle (b) for healthy individuals walking on ground slopes ranging from −6 deg (dark green) to +6 deg (light green) with level ground shown in a dashed line. Fig. 3a shows the ankle joint quasi-stiffness while Fig. 3b shows the ankle external quasi-stiffness. The gray band indicates the range of torque zero-crossings.

and external quasi-stiffness data (Fig. 3b). The RMSE for the internal quasi-stiffness data was 0.26 Nm/Kg while the RMSE for the external quasi-stiffness data was 0.14 Nm/Kg, indicating that the external quasi-stiffness model provides a better fit to a single consistent linear behavior across slopes. To further assess the degree to which the different quasi-stiffness models provide a consistent linear stiffness-like relationship across sloped walking conditions, the Pearson correlation coefficient was calculated for the internal and external quasi-stiffness data. The Pearson correlation coefficient was found to be −0.77 for the internal quasi-stiffness data and −0.94 for the external quasi-stiffness data, indicating that the external quasi-stiffness model provides a more consistent linear spring-like relationship across sloped walking conditions. In addition to these various statistical measures, the qualitative shape of the external quasi-stiffness curves is also consistent, exhibiting the behavior of a spring with an increasing and then decreasing stiffness.

These data provide evidence that external quasi-stiffness is maintained while walking across terrain with varying global slopes. The slope-adaptive controller presented here leverages this consistency to develop a single control policy that provides biomimetic walking behavior across varying ground slopes.

B. Controller Design

The overarching approach to providing slope adaptive behavior with a single control policy is to utilize a finite state machine controller to split the gait cycle into discrete phases as has been the approach in multiple prior works [9], [21], [52]. During the stance phase, however, the semi-powered ankle will emulate the consistent external quasi-stiffness observed

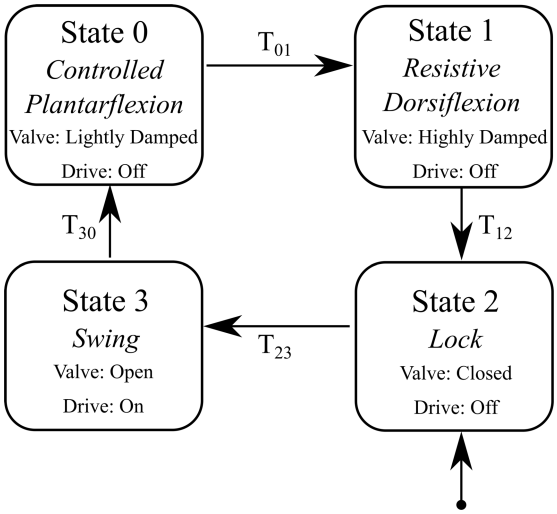

Fig. 4. Finite state machine for sloped walking consisting of four states and the transitions between them. The finite state machine also indicates the commanded state of the valve and drive motors during each state of the controller. Transition conditions are outlined in Table II.

in healthy subjects, thereby providing biomechanical behavior similar to that observed in healthy individuals independent of ground slope.

The design of the semi-powered prosthesis utilized in this work does not directly enforce an arbitrary shank-based set point and stiffness. Instead, the cylinder locks the ankle at a desired angle (by closing the hydraulic valve) to establish the set point of the ankle stiffness, while the stiffness is determined by the passive properties of the carbon fiber foot plate. Assuming the foot is flat on the ground, the value of the shank angle at which the hydraulic valve closes acts as the shank-based set point. As can be seen in Fig. 3, the set point of the external quasi-stiffness observed in healthy subjects is approximately zero deg (shank aligned with the gravity vector). As such, during the stance phase of walking, the hydraulic valve is closed when the shank is generally aligned with the gravity vector, thereby setting the shank-based equilibrium position. It should be noted therefore that in this system the timing of the ankle set point engagement is controllable by the prosthesis, while the stiffness behavior thereafter is determined by the passive design of carbon fiber foot plate (and at low torques, the series spring).The complete state machine utilized in the unified walking controller can be seen in Fig. 4. This finite state machine is similar to the one presented in [41] except that the one presented here incorporates the slope adaptive behavior described above. The transition conditions associated with the state machine depicted in Fig. 4 are outlined in Table II.

As seen in Fig. 4 and Table II, the state machine consists of four states: controlled plantarflexion (state 0), resistive dorsiflexion (state 1), lock (state 2), and swing (state 3). During each of these states, position commands are sent to the two motors in the actuator as indicated in Fig. 4. A stride begins at heel strike, when the controller is in the controlled plantarflexion state. During this state, the ankle is configured such that the damping valve provides the appropriate heel strike damping as the ankle conforms to the ground. Once

TABLE II
FINITE STATE TRANSITIONS FOR THE SLOPED WALKING CONTROLLER

Transition	Description	Condition
T_{01}	Shank has positive angular velocity as the foot is flat on ground	$\dot{\theta}_s > 0$ $\dot{\theta}_f \approx 0$ for $t > t_{th,01}$
T_{12}	Shank crosses virtual equilibrium position and has positive angular velocity	$\theta_s > \theta_{th,12}$ $\dot{\theta}_s > 0$
T_{23}	Ankle is unloaded	$\tau < \tau_{th,23_2}$ after $\tau < \tau_{th,23_1}$
T_{30}	Ankle has fully dorsiflexed	$\theta_a > \theta_{th,30}$

the shank angular velocity ($\dot{\theta}_s$) is positive and the foot is flat on the ground, as measured by near zero foot angular velocity ($\dot{\theta}_f$) for a short period of time (t), the controller transitions to the resistive dorsiflexion state (state 1). While in the resistive dorsiflexion state, the ankle provides a separately tunable level of damping that is typically higher than the damping from the previous state. Additionally, while in the resistive dorsiflexion state, the damping increases as the shank angle (θ_s) increases (becomes more aligned with the gravity vector). This gradual increase in damping allows the ankle torque trajectory to remain continuous in order to feel "smooth" to the user. Once the shank angle has reached a predefined threshold angle and the shank angular velocity is positive, the controller transitions into the lock state (state 2), at which point, the valve fully closes. During this state, the hydraulic actuator is locked, and the carbon fiber foot plate in series with the device dominates the ankle's dynamic behavior. The ankle exhibits this spring-like behavior during the stance phase of walking. Once the ankle has reached terminal stance, the ankle is unloaded as measured by the torque signal (τ). After the ankle is unloaded, the device moves into the swing state (state 3), at which point, the valve fully opens, and the ankle actively dorsiflexes in order to provide increased toe clearance during swing. Once the ankle angle (θ_a) has dorsiflexed past a threshold angle, the controller transitions back to the controlled plantarflexion state (state 0) in preparation for the subsequent heel strike.

This finite state machine controller was implemented in MATLAB/Simulink, and high-level control commands were sent to the embedded system via a control tether (all prosthesis power was provided by the onboard battery).

IV. EXPERIMENTAL ASSESSMENT

The semi-powered prosthesis was assessed in experiments with three transtibial amputee subjects (mean subject mass of 73 $\pm$ 12 Kg), who walked on slopes with the experimental prosthesis and with their respective daily-use prostheses. Approval to perform these experiments was granted by the Vanderbilt Institutional Review Board, and written informed consent was obtained from the subjects prior to the assessment.

The slope-adaptive controller was assessed relative to the subjects' daily-use prostheses (all commercially-available carbon fiber leaf spring devices) across a series of five slope conditions: 6 and 3 deg decline/incline (a positive slope angle will here forth indicate an incline while negative values will indicated a decline) as well as level ground. Each walking trial (conducted with both the semi-powered and daily-use devices) consisted of walking at 0.8 m/s for one minute on a split-belt instrumented treadmill. Acclimation periods were provided between the two prosthesis conditions. The walking speed and ground slopes chosen for this experiment were selected to match those assessed in [45].

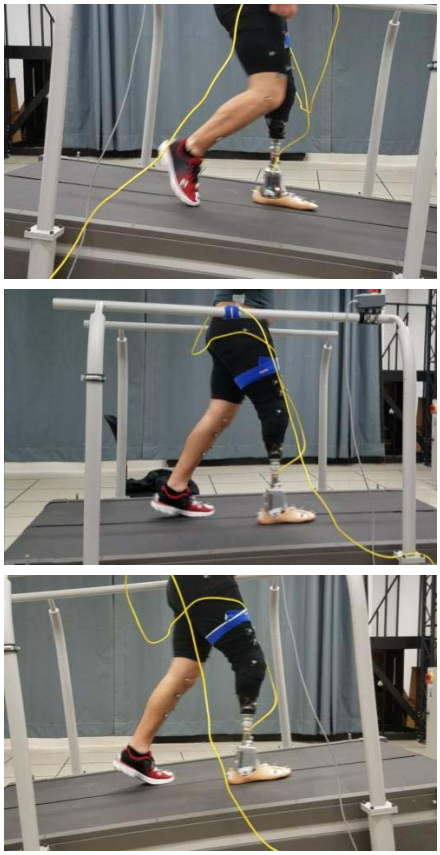

Fig. 5. Photos of subject walking with semi-powered prosthesis in the experimental setup on -6 deg, 0 deg, and 6 deg slopes.

During the experiments, ground reaction force data were collected under each foot at 1000 Hz using a split-belt instrumented treadmill (Bertec), and lower-body kinematics were recorded at 200 Hz via a synchronized motion capture system (Vicon). Photos of a subject using the semi-powered prosthesis in the experimental setup for the most extreme slopes and the level ground walking condition can be seen in Fig. 5. Biological joint angles, moments and powers were calculated over the stride using biomechanics modeling software (Visual 3D). All data were divided into strides normalized to 100% stride cycle, then averaged across strides prior to reporting.

In order to characterize the behavior of the semi-powered device, ankle angle, ankle torque, shank angle, toe clearance, and time between heel strike and foot flat during the stride were all calculated. These data were compared between the semi-powered ankle and the subjects' daily-use prostheses. Healthy subject data from [45] was utilized as a reference where possible.

The majority of these output metrics are directly reported from the biomechanics modeling software package (Visual 3D). Toe clearance was, however, calculated in post-processing based on the position of three markers corresponding to the plane of the treadmill and the position of a single point on

the ball of the foot. The Cartesian position of the point on the foot relative to the plane defined by the treadmill markers (using the corner of the treadmill as the origin) was calculated to indicate the trajectory of the ball of the foot across a stride. The time between heel strike and foot flat was calculated using video footage of the trials in which the subjects were walking on the steepest incline, steepest decline, and on level ground.

V. Results

In order to assess the degree to which the semi-powered ankle controller provides a consistent external quasi-stiffness equilibrium angle across varying ground slopes, body mass normalized ankle torque during middle stance was plotted against shank angle for the different ground slope conditions (averaged across all three subjects) as seen in Fig. 6. The slope associated with each trajectory in Fig. 6 is indicated by the shade of the trajectory where a lighter shade indicates a steeper incline. The consistency of the external quasi-stiffness equilibrium point was measured by the width of the band of initial torque zero-crossings (gray band in Fig. 6), which can be interpreted as the variance of external quasi-stiffness set points. This zero-crossing width was 5 deg for both the healthy and semi-powered ankle data and 12.5 deg for the passive daily-use device, which is unable to vary its set point. To assess the degree to which biomimetic ankle joint kinematic behavior is achieved by the prosthesis, the ankle joint angle (averaged across all three subjects) is shown in Fig. 7 for the two prosthesis conditions on the two most extreme slopes as well as level ground and is compared to averaged healthy ankle angle data.

To assess the degree to which the swing-phase dorsiflexion feature was able to provide ground clearance, the trajectory of a point on the foot (the point near the ball of the foot that is closest to the ground during swing phase) was tracked in the treadmill reference frame. The trajectory of this point on the foot was then averaged across all three subjects and plotted for both the semi-powered prosthesis condition as well as the passive daily use condition as seen in Fig. 8. This process was carried out for the most extreme slope conditions and the level ground walking condition. In Fig. 8, the positive X direction indicates the forward walking direction. The trajectories shown in Fig. 8 begin in the top right of the plot at heelstrike and continue in a clockwise direction throughout the duration of stride. As can be seen in Fig. 8a, the ground clearance trajectory may be slightly negative at times. This "ground penetration" is due to the flexing of the toes as well as the deformation of the foot cosmesis under loading. The large points marked on the trajectories in Fig. 8 indicate the instance of minimum foot clearance for their respective trajectories while the green dashed line indicates the mean minimum foot clearance for healthy subjects as reported in [53]. The minimum foot clearances in the level ground walking condition were 3.7 cm, 0.9 cm, and 1.4 cm for the semi-powered device, passive daily-use device, and healthy subjects, respectively.

The time between heelstrike and foot flat (time to foot flat) was also assessed, as shorter time to foot flat has been shown to increase perceived stability [54]. The conformal damping characteristics of the semi-powered ankle presumably enable

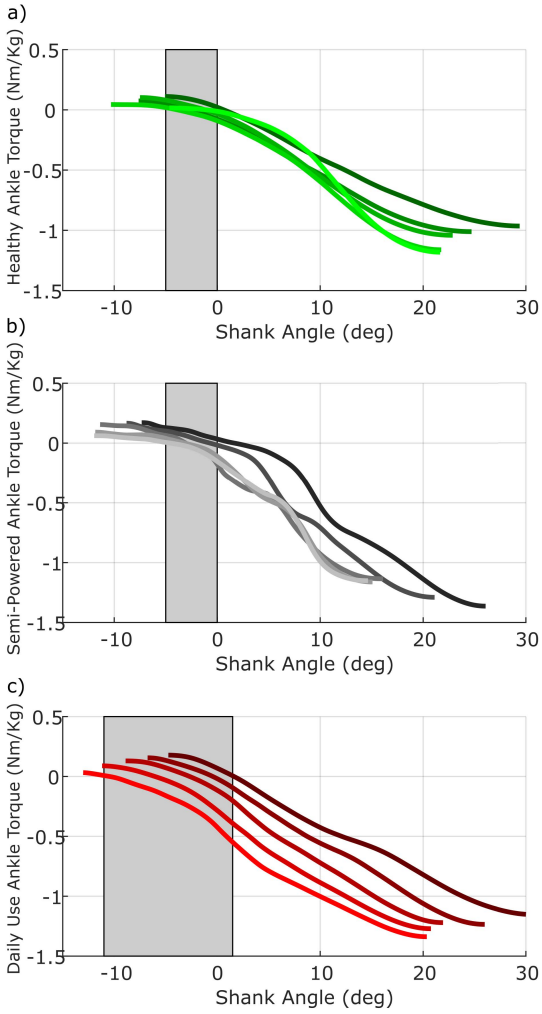

Fig. 6. Body-weight-normalized ankle torque plotted against shank angle for healthy subjects (a), the semi-powered ankle (b), and the passive daily-use device (c). The plotted data represent averages across multiple subjects The range of initial zero-torque crossings is highlighted as a gray bar. Lighter shades indicated steeper slope ascent.

reduced time to foot flat, relative to a conventional carbon fiber ankle/foot, which is limited in its ability to conform to the ground following heel strike. For the walking trials, the time to foot flat was averaged across subjects for the most extreme ground slope conditions as well as level ground while wearing the semi-powered device and daily-use prosthesis. The time-to-foot flat was also calculated for the subjects' sound side as a baseline. The results of this analysis can be seen in the bar plots shown in Fig. 9 in which error bars indicate +/− one standard deviation.

VI. Discussion

Fig. 6 depicts the degree to which the unified control policy was able to maintain a consistent external quasi-stiffness equilibrium point across the varying ground slopes (similar to the behavior of a healthy ankle). The trajectories in Fig. 6 begin at the left-most position on the plot and follow the curve from left to right. The torque zero crossing of each trajectory can be seen as the onset of the external quasi-stiffness behavior with the shank angle associated with that zero-crossing acting as the virtual set point of the spring-like behavior. Each trajectory

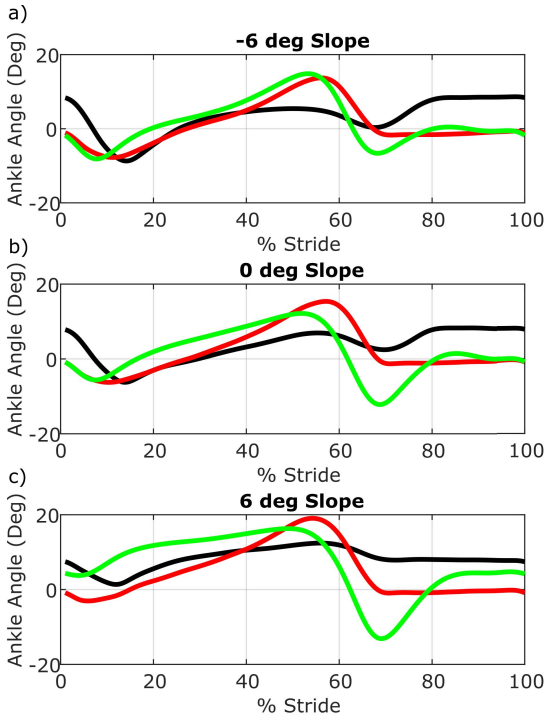

Fig. 7. Averaged ankle angle data for healthy subjects (green), the passive daily-use device (red), and the semi-powered device (black) while descending a 6 degree slope (a), walking on level ground (b), and ascending a 6 degree slope (c).

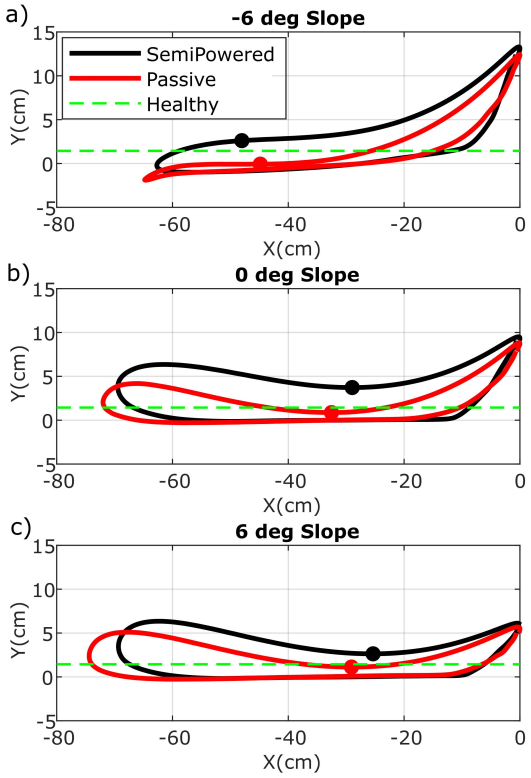

Fig. 8. Foot clearance trajectory (averaged across all subjects) in the laboratory frame for the semi-powered prosthesis and a passive daily-use device. The foot clearance trajectory is shown for the −6 deg (a), 0 deg (b), and 6 deg (c) ground slope conditions. Instances of minimum foot clearance are noted with a large dot. The green dashed line indicates the mean healthy subject minimum foot clearance for level ground walking.

in Fig. 6 represents a different ground slope condition, and as such, the range of torque zero-crossings represents the range of external quasi-stiffness set points adopted by the healthy ankle and prosthetic devices (range highlighted with gray band). As can be seen in Fig. 6, the healthy ankle and semi-powered device both have a narrow range of set points near shank angle of zero while the passive daily-use device exhibits a much wider (factor of two) range of set points. This shifting virtual set point associated with the passive device arises because the joint-angle-based set point of the prosthesis cannot change with the ground slope. It should also be noted that in the semi-powered device, the shape of the trajectory after the set point initiation is dominated by the dynamics of the carbon fiber leaf spring foot plate and series elastic element. As such, the "bumps" in the trajectories in Fig. 6b are likely due to the saturation of the series elastic element. In summary, healthy slope walking behavior is characterized by a shift in the joint-angle-based ankle stiffness equilibrium angle in such a manner that renders the "virtual" shank angle equilibrium essentially invariant, as shown in Fig. 6a. The controllable set-point of the semi-powered prosthesis enable it to provide this behavior, while the inability of the passive prosthesis to shift its ankle equilibrium angle prevents it from providing an invariant external quasi-stiffness equilibrium point.

The ankle angle data in Fig. 7 shows that the semi-powered ankle is providing appropriate ankle joint behavior across the various ground slope conditions. Specifically, the semi-powered ankle exhibits a distinct plantarflexion motion at heel strike, followed by dorsiflexion during stance. In late stance, energy is released from the series carbon fiber spring, and then during the swing phase, the ankle is actively repositioned to provide foot clearance. It may be noted from this data, however, that the semi-powered ankle did not dorsiflex as much as the healthy trajectory during the stance phase. This lack of dorsiflexion is largely due to the stiff carbon fiber foot plate utilized in this design, the passive dynamics of which dominate the stance phase. Future work will involve optimizing the design of this component to provide stance behavior more comparable to healthy data.

The foot clearance trajectory during level ground walking is shown in Fig. 8, and this figure shows that the semi-powered ankle obtains significantly more foot clearance as compared to the passive ankle prosthesis (a mean difference of 2.9 cm for the level ground walking condition). It should be noted that no significant differences in intact joint kinematics were identified when comparing the two prosthesis conditions, indicating that the difference in foot clearance is not likely to be a result of additional compensatory actions. Studies of healthy subjects indicate an average minimum foot clearance during level walking between 1 and 3 cm with a mean value of 1.4 cm [53]. The minimum foot clearance with the passive prosthesis is below the average healthy subject range, which may contribute to the higher incidence of falls and fear of falling that has been observed in the amputee population [6], [7], [55]. Similar foot clearance analysis was performed in [35] which showed that active dorsiflexion during the swing phase may reduce the likelihood of falls in the amputee population. The increased foot

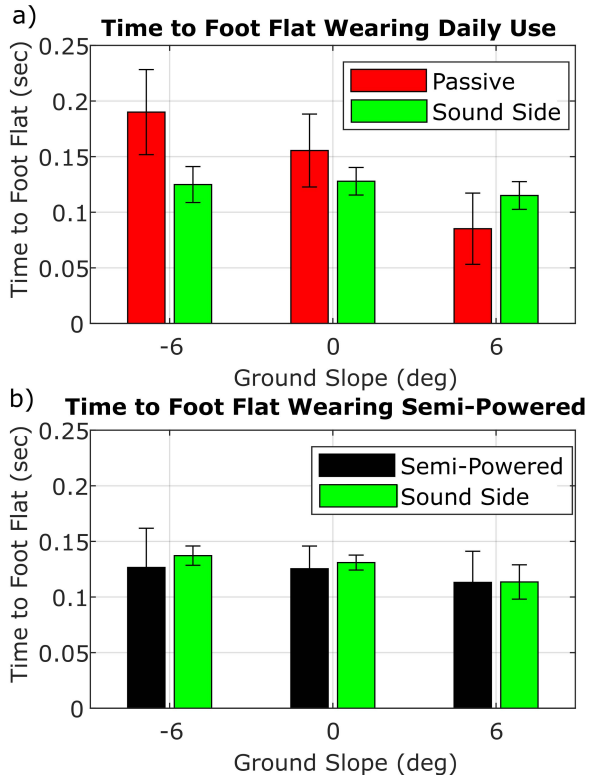

Fig. 9. Time to foot flat for the passive daily use device (red), the semi-powered device (black), and the subjects' sound side (green) across ground slope conditions ranging from −6 to 6 deg. Error bars indicate +/− one standard deviation. (a) shows the subjects' sound side time to foot flat while wearing their daily-use prosthesis while (b) shows the subjects' sound side time to foot flat while wearing the semi-powered device.

clearance observed while using the semi-powered prosthesis may help to decrease the likelihood of falls in this population.

Time to foot flat has been tied to perceived prosthesis stability [54]. The semi-powered device utilizes a controlled plantarflexion state in the control architecture in order to provide a consistent time to foot flat without exhibiting a "foot slap" behavior. The heelstrike behavior in the semi-powered prosthesis is characterized by a controlled damper whereas the heelstrike behavior of the daily-use device is that of a passive spring. The bidirectional capabilities of the constant volume actuator allows for the ankle's damping characteristics to be controlled during this plantarflexive state. As can be seen in Fig. 9a, the time to foot flat for the passive prosthesis is highly dependent on the ground slope, exhibiting longer times for downslopes than for upslopes. The semi-powered device, as well as the subjects' sound sides, exhibit a consistent and similar time to foot flat across all slopes. A comparison of Fig. 9a and 9b indicates that the semi-powered device promotes symmetry between the prosthetic and sound side with respect to time to foot flat. Fig. 9 indicates that the semi-powered device exhibits similar ground contact behavior to healthy ankles whereas passive prostheses may not.

VII. Conclusion

This paper describes a semi-powered ankle prosthesis, which is a substantially redesigned version of a previously presented version [40]. Unlike the previously presented device, the current device incorporates a unique constant volume hydraulic cylinder that enables the ankle to provide controlled damping and locking in a bidirectional manner. The semi-powered hardware design approach and novel actuator technology allow for a device with controllable repositioning and damping in a compact and lightweight package relative to fully powered prosthetic devices. A unified controller for level and sloped walking was developed based on observations of healthy ankle behavior and implemented on the redesigned ankle prosthesis. The prosthesis and unified controller were shown to better reproduce healthy ankle behavior across slopes, relative to a standard carbon fiber ankle. The ankle was also shown to provide some other potentially beneficial characteristics relative to the standard prostheses, including increased foot clearance during swing phase – resulting from active dorsiflexion during swing – and improved consistency in time to foot flat at heel strike – resulting from conformal damping during heel strike. Future work will include developing controllers for other activities and transitions between activities as well as comparisons to other prosthetic interventions.

References

[1] S. R. Koehler-McNicholas, E. A. Nickel, J. Medvec, K. Barrons, S. Mion, and A. H. Hansen, "The influence of a hydraulic prosthetic ankle on residual limb loading during sloped walking," *PLoS ONE*, vol. 12, no. 3, Mar. 2017, Art. no. e0173423.

[2] C. Gauthier-Gagnon, M.-C. Grisé, and D. Potvin, "Enabling factors related to prosthetic use by people with transtibial and transfemoral amputation," *Arch. Phys. Med. Rehabil.*, vol. 80, no. 6, pp. 706–713, Jun. 1999.

[3] C. Gauthier-Gagnon and M.-C. Grisé, "Tools to measure outcome of people with a lower limb amputation: Update on the PPA and LCI," *JPO J. Prosthetics Orthotics*, vol. 18, no. 6, pp. P61–P67, Jan. 2006.

[4] H. Burger, Č. Marinček, and E. Isakov, "Mobility of persons after traumatic lower limb amputation," *Disab. Rehabil.*, vol. 19, no. 7, pp. 272–277, Jan. 1997.

[5] B. Larsson, A. Johannesson, I. H. Andersson, and I. Atroshi, "The locomotor capabilities index; validity and reliability of the Swedish version in patients with lower limb amputation," *Health Qual. Life Outcomes*, vol. 7, no. 1, p. 44, 2009.

[6] W. C. Miller, A. B. Deathe, M. Speechley, and J. Koval, "The influence of falling, fear of falling, and balance confidence on prosthetic mobility and social activity among individuals with a lower extremity amputation," *Arch. Phys. Med. Rehabil.*, vol. 82, no. 9, pp. 1238–1244, Sep. 2001.

[7] W. C. Miller, M. Speechley, and B. Deathe, "The prevalence and risk factors of falling and fear of falling among lower extremity amputees," *Arch. Phys. Med. Rehabil.*, vol. 82, no. 8, pp. 1031–1037, Aug. 2001.

[8] L. E. Pezzin, T. R. Dillingham, E. J. MacKenzie, P. Ephraim, and P. Rossbach, "Use and satisfaction with prosthetic limb devices and related services," *Arch. Phys. Med. Rehabil.*, vol. 85, no. 5, pp. 723–729, 2004.

[9] S. Au and H. Herr, "Powered ankle-foot prosthesis," *IEEE Robot. Autom. Mag.*, vol. 15, no. 3, pp. 52–59, Sep. 2008, doi: 10.1109/MRA.2008.927697.

[10] A. H. Shultz, J. E. Mitchell, D. Truex, B. E. Lawson, and M. Goldfarb, "Preliminary evaluation of a walking controller for a powered ankle prosthesis," in *Proc. IEEE Int. Conf. Robot. Autom.*, May 2013, pp. 4838–4843.

[11] R. D. Bellman, M. A. Holgate, and T. G. Sugar, "SPARKy 3: Design of an active robotic ankle prosthesis with two actuated degrees of freedom using regenerative kinetics," in *Proc. 2nd IEEE RAS EMBS Int. Conf. Biomed. Robot. Biomechatronics*, Oct. 2008, pp. 511–516, doi: 10.1109/BIOROB.2008.4762887.

[12] J. Realmuto, G. Klute, and S. Devasia, "Nonlinear passive cam-based springs for powered ankle prostheses," *J. Med. Devices*, vol. 9, no. 1, Mar. 2015, Art. no. 011007.

[13] B. J. Bergelin, J. O. Mattos, J. G. Wells, and P. A. Voglewede, "Concept through preliminary bench testing of a powered lower limb prosthetic device," *J. Mech. Robot.*, vol. 2, no. 4, Nov. 2010, Art. no. 041005.

[14] P. Cherelle, V. Grosu, M. Cestari, B. Vanderborght, and D. Lefeber, "The AMP-foot 3, new generation propulsive prosthetic feet with explosive motion characteristics: Design and validation," *Biomed. Eng. OnLine*, vol. 15, no. S3, p. 21, Dec. 2016.

[15] M. Grimmer, M. Holgate, J. Ward, A. Boehler, and A. Seyfarth, "Feasibility study of transtibial amputee walking using a powered prosthetic foot," in *Proc. Int. Conf. Rehabil. Robot. (ICORR)*, Jul. 2017, pp. 1118–1123.

[16] M. Cempini, L. J. Hargrove, and T. Lenzi, "Design, development, and bench-top testing of a powered polycentric ankle prosthesis," in *Proc. IEEE/RSJ Int. Conf. Intell. Robots Syst.*, Sep. 2017, pp. 1064–1069.

[17] M. Wu, S. Thapa, M. R. Haque, and X. Shen, "Toward a low-cost modular powered transtibial prosthesis: Initial prototype design and testing," in *Proc. Design Med. Devices Conf.* New York, NY, USA: American Society of Mechanical Engineers, Apr. 2017, Art. no. V001T05A014.

[18] T. Yu, A. R. Plummer, P. Iravani, J. Bhatti, S. Zahedi, and D. Moser, "The design, control, and testing of an integrated electrohydrostatic powered ankle prosthesis," *IEEE/ASME Trans. Mechatronics*, vol. 24, no. 3, pp. 1011–1022, Jun. 2019.

[19] N. Thatte and H. Geyer, "Toward balance recovery with leg prostheses using neuromuscular model control," *IEEE Trans. Biomed. Eng.*, vol. 63, no. 5, pp. 904–913, May 2016.

[20] T. Elery, S. Rezazadeh, C. Nesler, J. Doan, H. Zhu, and R. D. Gregg, "Design and benchtop validation of a powered knee-ankle prosthesis with high-torque, low-impedance actuators," in *Proc. IEEE Int. Conf. Robot. Autom. (ICRA)*, May 2018, pp. 2788–2795.

[21] F. Gao, Y. Liu, and W.-H. Liao, "Implementation and testing of ankle-foot prosthesis with a new compensated controller," *IEEE/ASME Trans. Mechatronics*, vol. 24, no. 4, pp. 1775–1784, Aug. 2019.

[22] M. Carney, T. Shu, R. Stolyarov, J.-F. Duval, and H. M. Herr, "Design and preliminary results of a reaction force series elastic actuator for bionic knee and ankle prostheses," EngXiv, Tech. Rep., 2019, doi: 10.31224/osf.io/3wt5j.

[23] A. H. Shultz and M. Goldfarb, "A unified controller for walking on even and uneven terrain with a powered ankle prosthesis," *IEEE Trans. Neural Syst. Rehabil. Eng.*, vol. 26, no. 4, pp. 788–797, Apr. 2018, doi: 10.1109/TNSRE.2018.2810165.

[24] F. Sup, H. A. Varol, and M. Goldfarb, "Upslope walking with a powered knee and ankle prosthesis: Initial results with an amputee subject," *IEEE Trans. Neural Syst. Rehabil. Eng.*, vol. 19, no. 1, pp. 71–78, Feb. 2011.

[25] S. Culver, H. Bartlett, A. Shultz, and M. Goldfarb, "A stair ascent and descent controller for a powered ankle prosthesis," *IEEE Trans. Neural Syst. Rehabil. Eng.*, vol. 26, no. 5, pp. 993–1002, May 2018.

[26] B. Lawson, H. A. Varol, A. Huff, E. Erdemir, and M. Goldfarb, "Control of stair ascent and descent with a powered transfemoral prosthesis," *IEEE Trans. Neural Syst. Rehabil. Eng.*, vol. 21, no. 3, pp. 466–473, May 2013.

[27] A. J. Young, A. M. Simon, N. P. Fey, and L. J. Hargrove, "Intent recognition in a powered lower limb prosthesis using time history information," *Ann. Biomed. Eng.*, vol. 42, no. 3, pp. 631–641, Mar. 2014.

[28] J. D. Lee, L. M. Mooney, and E. J. Rouse, "Design and characterization of a quasi-passive pneumatic foot-ankle prosthesis," *IEEE Trans. Neural Syst. Rehabil. Eng.*, vol. 25, no. 7, pp. 823–831, Jul. 2017, doi: 10.1109/TNSRE.2017.2699867.

[29] M. K. Shepherd and E. J. Rouse, "The VSPA foot: A quasi-passive ankle-foot prosthesis with continuously variable stiffness," *IEEE Trans. Neural Syst. Rehabil. Eng.*, vol. 25, no. 12, pp. 2375–2386, Dec. 2017, doi: 10.1109/TNSRE.2017.2750113.

[30] F. Heremans, S. Vijayakumar, M. Bouri, B. Dehez, and R. Ronsse, "Bio-inspired design and validation of the efficient lockable spring ankle (ELSA) prosthesis," in *Proc. IEEE 16th Int. Conf. Rehabil. Robot. (ICORR)*, Jun. 2019, pp. 411–416.

[31] E. M. Glanzer and P. G. Adamczyk, "Design and validation of a semi-active variable stiffness foot prosthesis," *IEEE Trans. Neural Syst. Rehabil. Eng.*, vol. 26, no. 12, pp. 2351–2359, Dec. 2018.

[32] P. G. Adamczyk and I. F. Ekman Simões, "Prosthetic manipulator and method therefor," U.S. Patent 20 170 348 118, Feb. 25, 2020.

[33] T. Lenzi, M. Cempini, J. Newkirk, L. J. Hargrove, and T. A. Kuiken, "A lightweight robotic ankle prosthesis with non-backdrivable cam-based transmission," in *Proc. Int. Conf. Rehabil. Robot. (ICORR)*, Jul. 2017, pp. 1142–1147.

[34] A. R. Wu and A. D. Kuo, "Determinants of preferred ground clearance during swing phase of human walking," *J. Experim. Biol.*, vol. 219, no. 19, pp. 3106–3113, Oct. 2016.

[35] N. J. Rosenblatt, A. Bauer, D. Rotter, and M. D. Grabiner, "Active dorsiflexing prostheses may reduce trip-related fall risk in people with transtibial amputation," *J. Rehabil. Res. Develop.*, vol. 51, no. 8, pp. 1229–1242, 2014.

[36] A. R. De Asha, R. Munjal, J. Kulkarni, and J. G. Buckley, "Impact on the biomechanics of overground gait of using an 'Echelon' hydraulic ankle–foot device in unilateral trans-tibial and trans-femoral amputees," *Clin. Biomech.*, vol. 29, no. 7, pp. 728–734, Aug. 2014.

[37] D. E. Amiot *et al.*, "Development of a passive and slope adaptable prosthetic foot," in *Proc. 5A, 41st Mech. Robot. Conf.*, Aug. 2017, Art. no. V05AT08A066.

[38] E. Nickel, "Passive prosthetic ankle-foot mechanism for automatic adaptation to sloped surfaces," *J. Rehabil. Res. Develop.*, vol. 51, no. 5, p. 803, 2014.

[39] T. T. Sowell, "A preliminary clinical evaluation of the Mauch hydraulic foot-ankle system," *Prosthetics Orthotics Int.*, vol. 5, no. 2, pp. 87–91, Aug. 1981.

[40] H. L. Bartlett, B. E. Lawson, and M. Goldfarb, "Design of a power-asymmetric actuator for a transtibial prosthesis," in *Proc. Int. Conf. Rehabil. Robot. (ICORR)*, Jul. 2017, pp. 1531–1536.

[41] H. L. Bartlett, B. E. Lawson, and M. Goldfarb, "Design, control, and preliminary assessment of a multifunctional semipowered ankle prosthesis," *IEEE/ASME Trans. Mechatronics*, vol. 24, no. 4, pp. 1532–1540, Aug. 2019.

[42] J. T. Lee, H. L. Bartlett, and M. Goldfarb, "Design of a semipowered stance-control swing-assist transfemoral prosthesis," *IEEE/ASME Trans. Mechatronics*, vol. 25, no. 1, pp. 175–184, Feb. 2020.

[43] C. Rossa, J. Lozada, and A. Micaelli, "Design and control of a dual unidirectional brake hybrid actuation system for haptic devices," *IEEE Trans. Haptics*, vol. 7, no. 4, pp. 442–453, Oct. 2014.

[44] B. Johnson, H. Bartlett, and M. Goldfarb, "Design and characterization of a five-chamber constant-volume hydraulic actuator," *Int. J. Fluid Power*, vol. 20, no. 2, pp. 225–244, Nov. 2019.

[45] E. C. Honert and K. E. Zelik, "Foot and shoe responsible for majority of soft tissue work in early stance of walking," *Hum. Movement Sci.*, vol. 64, pp. 191–202, Apr. 2019.

[46] S. Habibi and A. Goldenberg, "Design of a new high performance electrohydraulic actuator," in *Proc. IEEE/ASME Int. Conf. Adv. Intell. Mechatronics*, Sep. 1999, pp. 227–232, doi: 10.1109/AIM.1999.803171.

[47] M. Linjama, H.-P. Vihtanen, A. Sipola, and M. Vilenius, "Secondary controlled multi-chamber hydraulic cylinder," in *Proc. 11th Scandin. Int. Conf. Fluid Power (SICFP)*, vol. 9, 2009, pp. 2–4.

[48] K. Heybroek and E. Norlin, "Hydraulic multi-chamber cylinders in construction machinery," in *Hydraulikdagarna*. Linköping, Sweden: Linköping Univ., Mar. 2015.

[49] W. Xiao-Ming, L. Qian, and L. Xin, "The four-chamber hydraulic cylinder," in *Proc. IEEE Int. Conf. Aircr. Utility Syst. (AUS)*, Oct. 2016, pp. 686–689.

[50] H. Bartlett, "A symmetric multichamber hydraulic cylinder with variable piston area: An approach to compact and efficient electrohydrostatic actuation," *J. Mech. Design*, pp. 1–35, Dec. 2020.

[51] J. Ahn, D. Kim, S. Bang, N. Paine, and L. Sentis, "Control of a high performance bipedal robot using viscoelastic liquid cooled actuators," 2019, *arXiv:1906.03811*. [Online]. Available: http://arxiv.org/abs/1906.03811

[52] F. Sup, H. A. Varol, J. Mitchell, T. J. Withrow, and M. Goldfarb, "Preliminary evaluations of a self-contained anthropomorphic transfemoral prosthesis," *IEEE/ASME Trans. Mechatronics*, vol. 14, no. 6, pp. 667–676, Dec. 2009, doi: 10.1109/TMECH.2009.2032688.

[53] R. Begg, R. Best, L. Dell'Oro, and S. Taylor, "Minimum foot clearance during walking: Strategies for the minimisation of trip-related falls," *Gait Posture*, vol. 25, no. 2, pp. 191–198, Feb. 2007.

[54] M. J. Major, M. Twiste, L. P. J. Kenney, and D. Howard, "The effects of prosthetic ankle stiffness on stability of gait in people with transtibial amputation," *J. Rehabil. Res. Develop.*, vol. 53, no. 6, pp. 839–852, 2016.

[55] W. C. Miller, A. B. Deathe, and M. Speechley, "Lower extremity prosthetic mobility: A comparison of 3 self-report scales," *Arch. Phys. Med. Rehabil.*, vol. 82, no. 10, pp. 1432–1440, Oct. 2001.